EFFECT OF MEMBRANE THICKNESS AND UNSATURATION ON DYE EFFLUX RATES INDUCED BY δ-LYSIN FROM PHOSPHATIDYLCHOLINE VESICLES

Diana Wu

A Thesis Submitted to the
University of North Carolina Wilmington in Partial Fulfillment
Of the Requirements for the Degree of
Master of Science

University of North Carolina Wilmington

2005

Approved by

Advisory Committee

Ned Martin

Stephen Kinsey

Paulo Almeida
Chair

Accepted by

_____
Dean, Graduate School

This thesis has been prepared in the style and format

consistent with the journal

Biochemistry

TABLE OF CONTENTS

ABSTRACT

An important region of the cellular membrane that appears to have major influence on membrane-peptide interactions is the hydrophobic acyl chain region. In this study two lipid series were used to determine whether specificity towards membranes is influenced by acyl chain length, or membrane thickness, or by the degree of acyl chain unsaturation. Additionally, this quantitative investigation also provided insight on the effects of free volume and bilayer elasticity. The interaction of the peptide δ-lysin, a 26-residue peptide, to lipid bilayers was studied using stopped-flow fluorescence. Samples of carboxyfluorescein filled vesicles of various lipid concentrations were mixed with δ-lysin resulting in dye efflux. The experimental curves of carboxyfluorescein efflux as a function of time were measured at lipid concentrations ranging from 12.5 μM to 200 μM.

Constant τ values were calculated to determine the weighted average of the relaxation times of each carboxyfluorescein release function. It was found the main cause for dye efflux was a thinner membrane. Also, bending of the membrane was found to be dependent on the thickness of the bilayer. The stretching ability of the membrane had less significance in peptide insertion. As a result of bending stiffness being a major factor for peptide insertion, it appears that δ-lysin binds to the surface of the membrane due to the hydrophobic effect, and sink as a 'wedge' into the lipid bilayer.

ACKNOWLEDGEMENTS

I would like to thank Dr. Paulo Almeida and Dr. Antje Almeida for taking me under their wing. Without your generosity for allowing me to join your lab, this would never have been possible. Thank you to my committee members, Dr. Martin and Dr. Kinsey for your guidance. Thanks to my professors in the Chemistry department. I have an appreciation to this field because of your willingness to share knowledge and experience.

To my family, I thank you very much for supporting me throughout my education. Dad, I'm so glad to share this subject of interest with you. Mom, your meals were a lifesaver. Mike, you are my biggest fan and I am eternally grateful. I love you all.

Thank you to Jenny Wright for being there with me the whole way. Thanks to Lindsay Yandek for keeping me sane.

Thanks to my lab mates, Monica Lassiter, Lexi Oldham, and Sonia Gregory for all the good conversations.

Finally, thanks to my mentors and friends Dr. Kirk Brown, Aaron Wilcox, Dr. Jack and Doris Levy, and Mary Gornto.

LIST OF TABLES

Table Page

LIST OF FIGURES

INTRODUCTION

Antimicrobial peptides are an ancient form of defense developed by organisms over several millions of years to protect themselves against bacteria, fungi, and viruses (1). They have been found in many species including insects, amphibians, and humans (2), as well as in plants (3). Most of these peptides are short polypeptide sequences that range from 12-50 residues (4) and are derivatives of larger precursors (3). With an increasing number of antibiotic-resistant bacteria, the search to discover new, more effective ways to combat microorganisms has become increasingly important. In fact, for more than thirty years there has been an absence of new drugs until the recent release of the streptogramins, synercid, and oxazolidinone linezolid (5). However, it is only a matter of time before new strains of bacteria become resistant to these antibiotics, thus rendering them obsolete. Antimicrobial peptides appear to possess advantages over traditional antibiotics; there are an endless number of structures to study and resistance is not easily developed (5).

According to a review by Matsuzaki (6), antimicrobial peptides must follow four main criteria to be useful. They must be selectively toxic, fast killing, possess broad antimicrobial spectra, and there should be no resistance development. Peptides are classified as cationic or anionic of eukaryotic origin, and cationic, neutral, and anionic of prokaryotic origin (1). Several models have been proposed for the mechanism of function of these peptides. The *barrel-stave* model is considered the "classical picture" to describe pore formation. It requires that the peptides assemble on the membrane surface before pore formation, followed by insertion into the hydrophobic core of the membrane where it forms a pore. The *toroidal hole* or *wormhole model* is a modified version of the barrel stave model, but it functions at high peptide concentrations for predominantly hydrophobic sequences (6). Peptides insert into the membrane inducing a high

curvature folding where the inner leaflets and outer leaflets communicate. A third model, called the *carpet model*, has been used to describe surface-acting peptides that bind to the surface of the membrane in a 'carpet-like manner,' causing the membrane to disintegrate. Membrane permeation occurs when there is a high concentration of membrane-bound peptides that align on the membrane surface and bind to the headgroups of phospholipids, but they are not inserted into the hydrophobic core. Instead, the hydrophobic residues rotate towards the hydrophobic core causing disintegration of the membrane (7). A fourth model, operating through a *detergent-like effect*, proposes that the peptides cover the bilayer to disintegrate the membrane barrier similar to that of a detergent (2). The in-plane diffusion model describes cell death via low peptide-to-lipid ratios. Curvature strain is imposed by intercalated amphipathic peptides and the lipid packing is disturbed, which form transient openings (2). Finally, the *sinking raft* model works by forming side-by-side aggregates that adhere to the membrane forming a raft. Afterwards, the aggregates sink into the outer bilayer leaflet like a sinking raft. Consequently, cavities are formed in the most unstable intermediate states where leakage of vesicle contents can occur (8).

Despite the research so far, the mechanism of cell specificity is still not well understood. What is known is that the peptide must come in contact with the membrane first, before it can initiate cell death. Studies of both D and L enantiomers of the same peptides have been performed on membranes; both work equally effectively, suggesting that cell-surface receptors are not responsible for peptide action. Instead, direct peptide-lipid interaction may be the underlying mechanism (2, 9).

Since the lipid bilayer is the first point of contact, the peptide may use the bilayer surface to discriminate between certain cell types over others (8). In addition, the cell surface should be preferably the site of action for rapid cell killing rather than the cell interior (6). Most

antimicrobial peptides are cationic. The net positive charge is electrostatically attracted to the bacterial membranes because they have high amounts of negatively charged phospholipids, such as phophatidylglycerol (PG) (6). However, not all peptides are attracted to the membrane exclusively due to charge. The peptide Cecropin A has been shown to possess a strong affinity to the lipid bilayer; it also appears to have a dependence on the fatty acyl chain length in that the binding isotherm for 1-palmitoyl-2-oleoyl-*sn*-glycero-3-phosphatidylcholine (POPC)/1-palmitoyl-2-oleoyl-*sn*-glycero-3-pohosphatidylglycerol (POPG) vesicles display a characteristic cooperativity suggesting self-associated peptide monomers in the bilayer (10).

Another region of the phospholipid bilayer that appears to have major influence on membrane-peptide interactions is the hydrophobic acyl chain region. Numerous observations have been made regarding the effect of the degree of unsaturation of the acyl chain on peptide function. In one study, the secondary structure of melittin changed considerably by the loosening of inter-phospholipid packing near the lipid-water interface due to an increase of unsaturation in membranes (11). It is well established that aqueous, monomeric melittin shows essentially a random coil conformation; however, membrane-bound melittin shows a CD spectra of an α-helical conformation (11). Another study found that an increase of acyl chain unsaturation resulted in an alteration of acyl chain packing in the gel phase causing a decrease in melittin-induced micellization (12). Pore formation was reduced in the presence of *cis* unsaturation on each acyl chain (13). Rawicz *et al.* (14) found that increase in lipid unsaturation led to a reduction in bending stiffness due to a decrease in membrane thickness of the bilayer. In addition to the conclusions made by these studies, two separate investigations noted observations in relation to chain length (14, 15). The conclusions reached by these studies have brought attention to the hydrophobic region of the membrane, but they were made as additional

observations to the main investigation of that particular study conducted. No definitive conclusions could be made for the effect of membrane thickness and unsaturations on peptide function at this time mainly because too few lipids have been examined, or these studies only performed a qualitative analysis. The question that is addressed in this study is whether specificity towards membranes is influenced by acyl chain length, or membrane thickness, or by the degree of acyl chain unsaturation. Only a quantitative study with a series of related lipids can answer this question.

δ-Lysin is a 26-residue amphipathic peptide produced by the bacterium *Staphyloccoccus aureus* (8). It is an amphipathic peptide because, when it forms an alpha-helix, approximately one face of the helix is hydrophobic and the other face is hydrophilic (Figure 1).

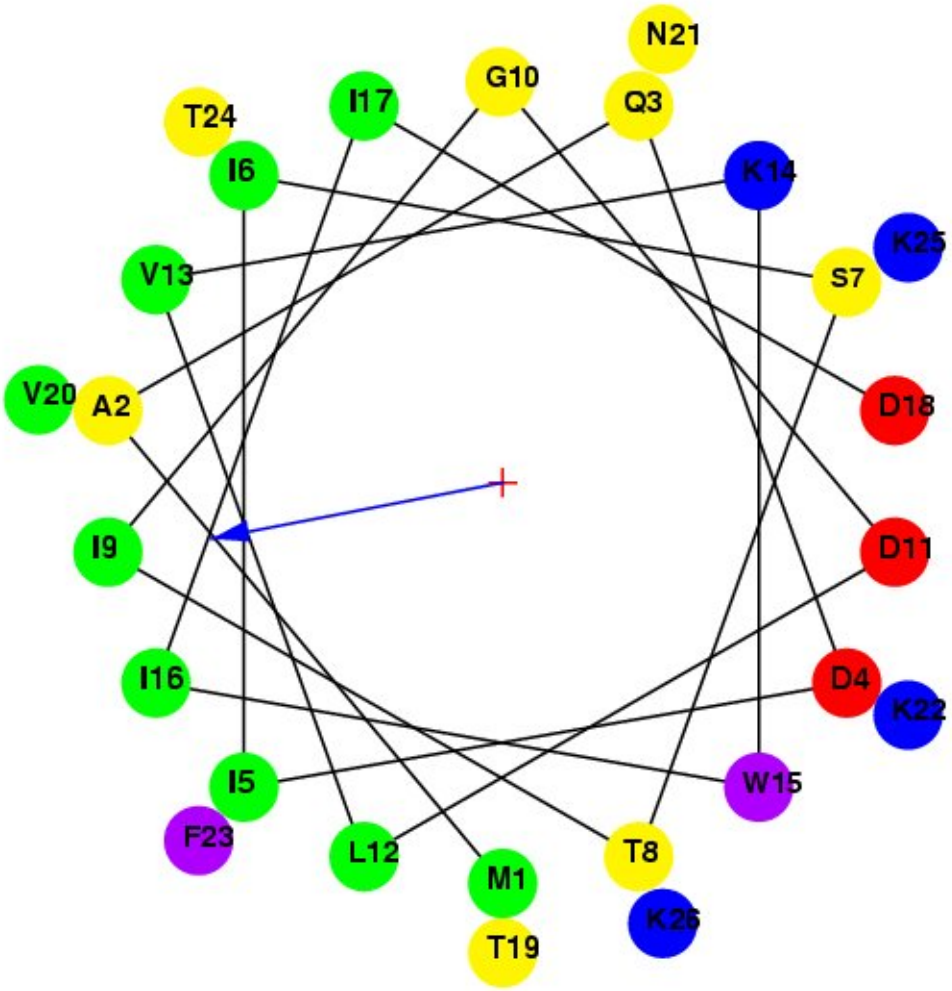

FIGURE 1: Helical wheel projection of δ-lysin. The green circles represent the hydrophobic face of δ-lysin and the arrow points towards the center of the hydrophobic region. All other colors are hydrophilic amino acids. The numbers show the order of the amino acid sequence.

In this conformation, it binds to membranes, similarly to many other peptides due to the hydrophobic effect. However, unlike many other peptides that are cationic and therefore bind well to negatively charged bacterial membranes, δ-lysin binds to neutral membranes as well (8). δ-Lysin interacts well with phosphatidylcholine (PC) lipids, and it appears that charge is not the mechanism of specificity, because the binding process does not seem to require a specific charge on the membrane surface (8). It was traditionally thought that a negative charge on the membrane was required in order for cationic peptides to bind (8). With several studies supporting acyl chain length composition as a factor that influences peptide behavior, it was necessary to investigate the effect of acyl chain length dependence on the action of the peptide in detail.

It was predict that the interaction between the peptide and the acyl chain determines the size of the peptide aggregate necessary for membrane perturbation by the creation of a pore of adequate size. This hypothesis is divided into two sub-hypotheses, which incorporate the effects of free volume and bilayer elasticity. According to the free volume theory, the probability to form a hole increases with free volume (v_f), which is the void created by fluctuations in density or redistribution of particles, and decreases exponentially with the required hole size (v^*) (16, 17).

$$P(v^*) = exp\ (-\gamma v^*/v_f) \tag{1}$$

The free volume is dependent on temperature (Vaz *et al.*, 1985) by the equation:

$$vf = \alpha + \beta\ (T - T_m) \tag{2}$$

where T is the experimental temperature and T_m is the phase transition temperature of the lipid bilayer. Varying acyl chain length in the lipid series diC14:1PC, diC16:1PC, diC18:1PC,

diC20:1PC, and diC22:1PC, at constant temperature, corresponds to varying T_m. If free volume were the dominating factor for membrane disruption, then v_f should vary little, because lipid lateral diffusion coefficients do not vary significantly for this lipid series (19). We studied a second series, diC18:1PC, diC18:2PC, and di18:3PC, which provides insight into the role of bilayer elasticity. Along with other unsaturated PCs, as the degree of unsaturations increases, the elastic stretch modulus decreases (14). Both lipid series are expected to change little for v_f, but they do vary the bilayer thickness. If bilayer elasticity rather than free volume is the determinant factor for peptide insertion, then the rate of dye efflux should increase as the membrane thickness decreases. Dye efflux rate increase should be more pronounced in the polyunsaturated series because they have thin bilayers. If instead there were a greater variance for free volume, this would suggest a stronger dependence on aggregate size.

MATERIALS AND METHODS

Chemicals

Phosphotidylcholine lipids were purchased in chloroform from Avanti Polar Lipids, Inc. Carboxyfluorescein was obtained from Fluka (Sigma-Aldrich Group, Spain). Lipids were used without further purification.

Preparation of Large Unilamellar Vesicles (LUV)

Individual solutions of phosphotidylcholine lipids suspended in chloroform were placed in a round-bottomed flask, and the solvent was evaporated using a rotary evaporator (Büchi R-3000) at 60˚ and placed in a desiccator for four hours to evaporate any remaining trace of chloroform. The lipid film was hydrated using filtered carboxyfluorescein buffer with a composition of 50 mM carboxyfluorescein, 20 mM MOPS, 0.1 mM EGTA, pH 7.5, 0.02 % NaN_3 to give a final lipid concentration of 10 mM. The mixture was vortexed for five minutes until a turbid suspension of multilamellar vesicles was visible, which was subsequently freeze-thawed five times with liquid nitrogen to create osmotic balance between the bilayers. This process was followed by extruding the lipid suspension 10 times through two 0.1 μm stacked Nucleopore polycarbonate filters. The extrusion was performed using a water jacket high-pressure extruder from Lipex Biomembranes Inc. Afterwards, the LUV were passed through a Sephadex G-25 column using 20 mM MOPS, 100mM KCl, 0.1 mM EGTA, pH 7.5, and 0.02 % NaN_3 buffer, to separate carboxyfluorescein in the buffer external from the lipid vesicles containing encapsulated carboxyfluorescein. A modified version of the phosphate assay (Bartlett, 1959) was then performed where appropriate volumes of samples and standards were pipetted, and the volume adjusted to 300 μL with distilled water. After the addition of 700 μL of $HClO_4$, all tubes were covered with marbles and placed in a heating block at 200˚C until clear.

Once the tubes cooled, 2 mL of a 1% solution of ammonium molybdate were pipetted to each tube followed by 2 mL of a 4% solution of ascorbic acid. The tubes were then placed in a water bath for 30 min, and the absorbance was read at 580 nm.

Fluorescence Experiments

The rate of dye efflux was measured with an SLM-Aminco 8100 spectrofluorometer. A stopped-flow unit from Applied Photophysics RX2000 Rapid Kinetics was attached to the fluorometer with a cuvette placed in the SLM. Two syringes on the stopped-flow unit housed separate chambers for 1 μM of peptide in 1mL of 100 mM KCl, and vesicles in a solution of MOPS buffer composed of 20 mM MOPS, 100 mM KCl, 0.1 mM EDTA, pH 7.5, and 0.02 % NaN_3 buffer. Concentrations of lipid varied from 25 – 200 μM.

The peptide solution was adjusted to a pH of 3. The acidic conditions kept the peptide protonated, which caused the peptides to have the same charge. The like charges would repel and therefore prevent peptide aggregation in solution. Potassium chloride was included to keep the vesicles in osmotic balance after mixing with peptide. The peptide monomers had a high affinity for the membrane due to the hydrophobic effect. Under these conditions, upon mixing of peptide and vesicle solutions a kinetic trace was measured and analyzed.

Data Analysis

τ values were calculated for all kinetic traces. The τ represents the weighted average relaxation time (characteristic time) of each carboxyfluorescein release function. $f(t)$ is the time derivative of the dye efflux as a function of time (release function), measured by the increase in carboxyfluorescein fluorescence.

$$\tau = \frac{\int_0^\infty t f(t)\, dt}{\int_0^\infty f(t)\, dt} \qquad (3)$$

RESULTS

Carboxyfluorescein efflux from Phosphotidylcholine Vesicles

The experimental curves of carboxyfluorescein efflux as a function of time were measured at lipid concentrations ranging from 12.5 μM to 200 μM while the peptide concentration was kept constant throughout all experiments at 0.5 μM. Lipid concentrations of 12.5 μM through 100 μM were measured for lipids with efflux rates that were very slow relative to other lipids, such as diC18:2PC. Fluorescence was measured by excitation at 470 nm and emission at 520 nm. Curves for all 50μM lipid concentrations are shown in Figure 2 and Figure 3 for each lipid in both series. These curves show that an increase in lipid acyl chain length results in a decrease of dye efflux rates. The fastest rate was observed for diC14:1PC and the slowest for diC22:1PC. Also evident from the curves was the correlation between lipid concentration and the rate of dye efflux. Dye efflux rates decreases as lipid concentration increased. This is indicated in Table 1, which shows the values of the average characteristic times of dye efflux (τ) for all lipids examined. Table 1 shows calculated τ values determined by the equation shown on page 10.

Table 1 Average τ values and standard deviations for unsaturated lipids. τ values increase with acyl chain length and decrease with chain unsaturation for each lipid concentration. Also observed was a decrease in dye efflux rate with increasing lipid concentration, for each lipid.

Lipid	$\tau_{12.5\ \mu M}$	±SD	$\tau_{25\ \mu M}$	±SD	$\tau_{50\ \mu M}$	±SD
14:1	--	--	1.1	0.1	1.6	0.20
16:1	--	--	5.6	5.6	64	31
18:1	--	--	71	16	1400	100
18:2	52	5.2	38	37	290	140
18:3	--	--	17	7.1	180	43
20:1	18	0.76	130	160	2000	1400
22:1	630	930	9200	3800	14000	1100

Lipid	$\tau_{100\ \mu M}$	±SD	$\tau_{200\ \mu M}$	±SD
14:1	3.2	1.6	120	0
16:1	180	64	620	130
18:1	4400	1400	9100	0
18:2	--	--	--	--
18:3	560	180	1100	180
20:1	6400	2000	--	--
22:1	--	--	--	--

Dye efflux rate for the lipid diC14:1PC occurred very rapidly and was noisier compared to longer acyl chain lengths because of the small concentration of encapsulated carboxyfluorescein. It was important to perform experiments for diC14:1PC prior to the lipid concentration assay due to the rapid leakage of the vesicles. Lipids with other acyl chain lengths in this series did not require immediate testing because they encapsulated the dye more successfully and retained it far much longer in the absence of peptide. Leakage of the dye from the vesicles was apparent when the sample was fluorescent rather than pale yellow, prior to addition of δ-lysin. Carboxyfluorescein is a self-quenched dye at high concentrations. It fluoresces only when diluted, such as when concentrated carboxyfluorescein escaped into the buffer medium.

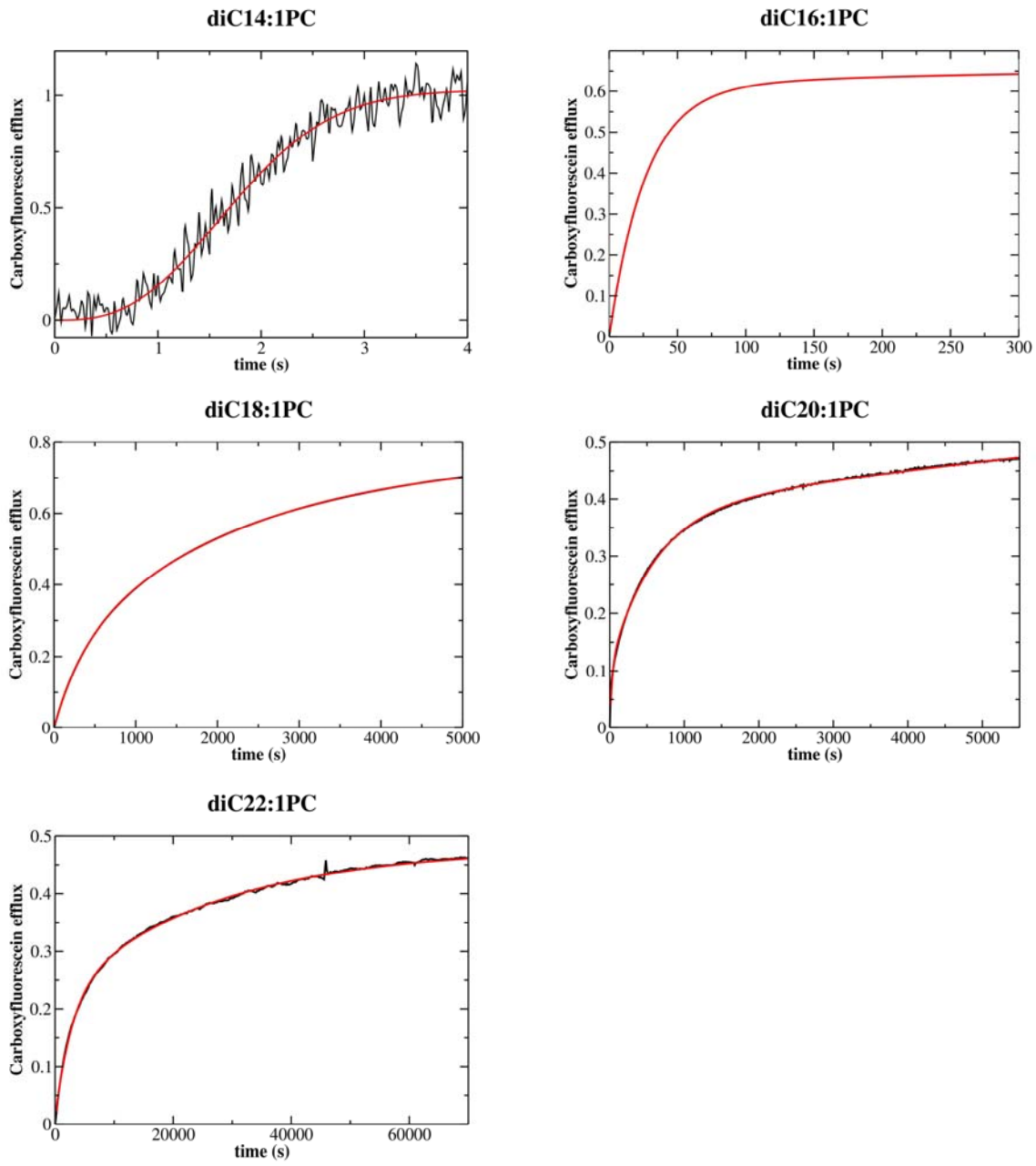

FIGURE 2. Carboxyfluorescein efflux as a function of time. Y axis is fraction of total dye efflux. The maximum possible amount of efflux was determined by lysis of the vesicles with the detergent Triton X-100. Series diC14:1PC, diC16:1PC, di18:1PC, di20:1PC, and di22:1PC at 50 μM. The sequence of panels shows the effect of increasing chain length by the addition of two carbons to each acyl chain length on the rate of dye efflux. The rate decreased (τ increased) as chain length increased.

Figure 3 shows the results for the second series of lipids at 50 μM. In this series diC18 chain lipids were used to make vesicles, each lipid differing from the previous one by an addition of one unsaturation per acyl chain. As shown in Figure 3, the time spans (τ) for each curve became shorter as the number of unsaturations increased. Table 1 shows the τ values for this series. DiC18:1PC had a τ of 1400 ± 100 s; however, with an addition of just one unsaturation to each acyl chain a τ value of 190 ± 140 s was obtained. Adding yet another unsaturation to the acyl chain showed a less dramatic decrease in the τ value which was calculated to be 180 ± 43 s. There appears to be a threshold at which the membrane is more susceptible to peptide attack. It seems that with one unsaturation per acyl chain the membrane is quite resilient to δ-lysin. However, when there are two unsaturations per acyl chain the dye efflux appears to be dramatically faster. Two other lipids were used to prepare vesicles but we were not successful in forming vesicles that encapsulated carboxyfluorescein for a long enough period of time to perform experiments. These lipids were diC20:4PC and diC22:6PC. We believe that it may not be feasible to form dye-encapsulated vesicles of these highly unsaturated lipids.

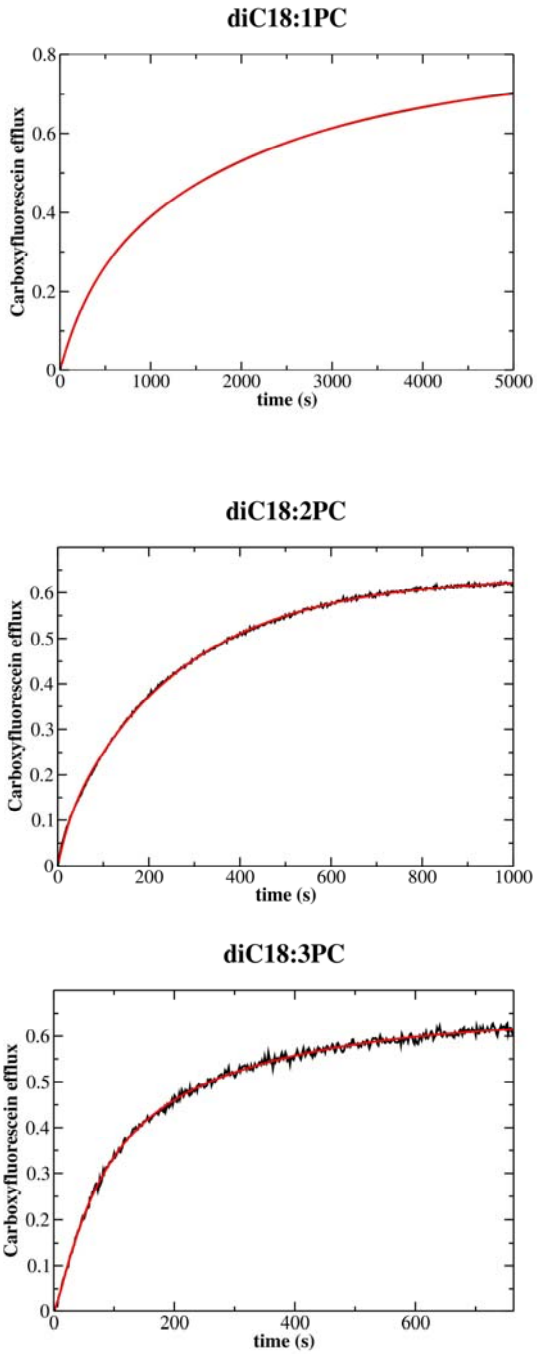

FIGURE 3. Carboxyfluorescein release from vesicles composed of the lipid series diC18:1PC, diC18:2PC, and di18:3PC at 50 μM. Y axis is percentage of total dye efflux. The sequence of panels shows the effect of increasing acyl chain unsaturation to each acyl chain on the rate of dye efflux. The rate increased (τ decreased) as acyl chain unsaturation increased.

Apparent permeability values obtained from Olbrich *et al.* (15), which are given in Table 2, show very little indication as to why τ values changed dramatically between diC18:1PC and diC18:2PC lipids. Instead values for elastic and bending moduli values obtained from Rawicz *et al.* (14), shown in Tables 3 and 4, help to explain better why there was a change in the rate of dye efflux. Between diC18:1PC and diC18:2PC the elastic modulus (K_A) decreases more than between diC18:2PC and diC18:3. K_A is 270 ± 18 mN/m for diC18:1PC and decreases to 250 ± 21 mN/m for diC18:2PC, whereas diC18:3PC has a K_A value of 240 ± 32 mN/m. Similarly, the bending moduli (K_c) values follow a similar trend with diC18:1PC having a K_c of 0.85 x 10^{-19} J, diC18:2PC of 0.44 x 10^{-19} J, and diC18:3 of 0.38 x 10^{-19} J. The bending modulus of diC18:2PC is nearly half that of diC18:1PC.

Table 2 Apparent permeability to water. Data taken from Olbrich (15). Permeability increases with the number of unsaturations on the acyl chain.

Lipid	P_{fapp} (μm/sec)
18:1	42 ± 6
18:2	91 ± 24
18:3	146 ± 26

Table 3 Elastic moduli K_A for fluid phase bilayers. Data taken from Rawicz (14). K_A decreases minimally with increasing number of unsaturations.

Lipid	K_A (mN/m)
18:1	265 ± 18
18:2	247 ± 21
18:3	244 ± 32
22:1	263 ± 10

Table 4 Bending moduli k_c for fluid phase bilayers. Data taken from Rawicz (14). k_c decreases more obviously with increasing unsaturation, especially between one and two unsaturations.

Lipid	k_c (10^{-19}J)
18:1	0.85 ± 0.10
18:2	0.44 ± 0.07
18:3	0.38 ± 0.04
22:1	1.20 ± 0.15

Figure 4 shows results for τ plotted against all chain lengths in the first lipid series. This graph gives some indication on the trend of aggregate size. The plot shows a steep positive slope starting from 12.5 μM until 50 μM lipid. This indicates that δ-lysin acts more effectively to release dye at lower lipid concentrations up until 50 μM lipid. DiC14:1PC vesicles appear to have the slowest ascent for initial slope at those concentrations. At 50 μM through 100 μM lipid the τ increase is smaller, as shown by a smaller slope for all chain lengths except diC14:1PC. Also, τ values for diC18:2PC and diC20:1PC are very close between lipid concentrations from 25 μM through 100 μM. Beyond 100 μM, τ values for all lipid chain lengths appear to level off with the exception of diC22:1PC, which levels off at 25 μM.

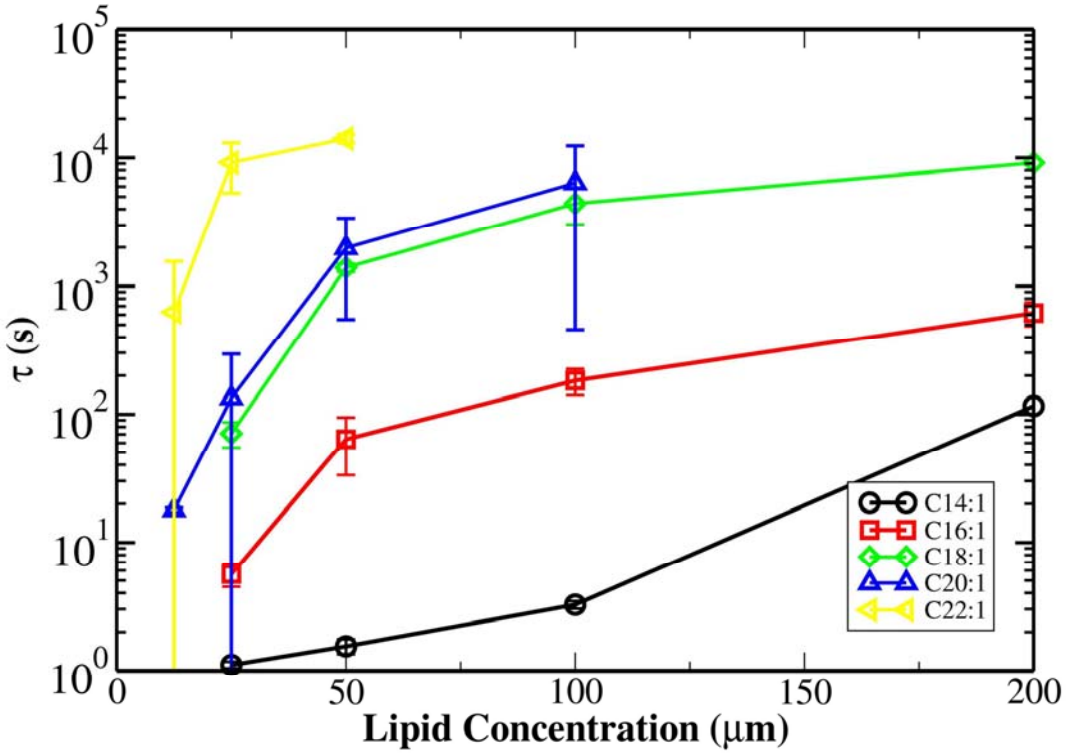

FIGURE 4: The effect of lipid concentration on carboxyfluorescein efflux shown by plotting against average τ for all chain lengths of first lipid series.

The corresponding plot for the series diC18:1PC, diC18:2PC, diC18:3PC is shown in Figure 5. There is a more gradual increase in τ for all diC18 unsaturated lipids compared to the previous graph. It is noticeable that the initial slopes are similar to each other as the lipid concentration doubles from 25 μM to 50 μM, unlike the previous graph where diC14:1PC did not seem to follow the trend along with other chain lengths in the first series. τ for diC18:1PC and diC18:3PC appear to level off at about 100 μM. With constant peptide concentration, this is essentially the same as altering the peptide concentration on the membrane surface. In other words, as the lipid concentration increases, the peptide on the membrane surface is diluted out because there are fewer peptides per vesicle.

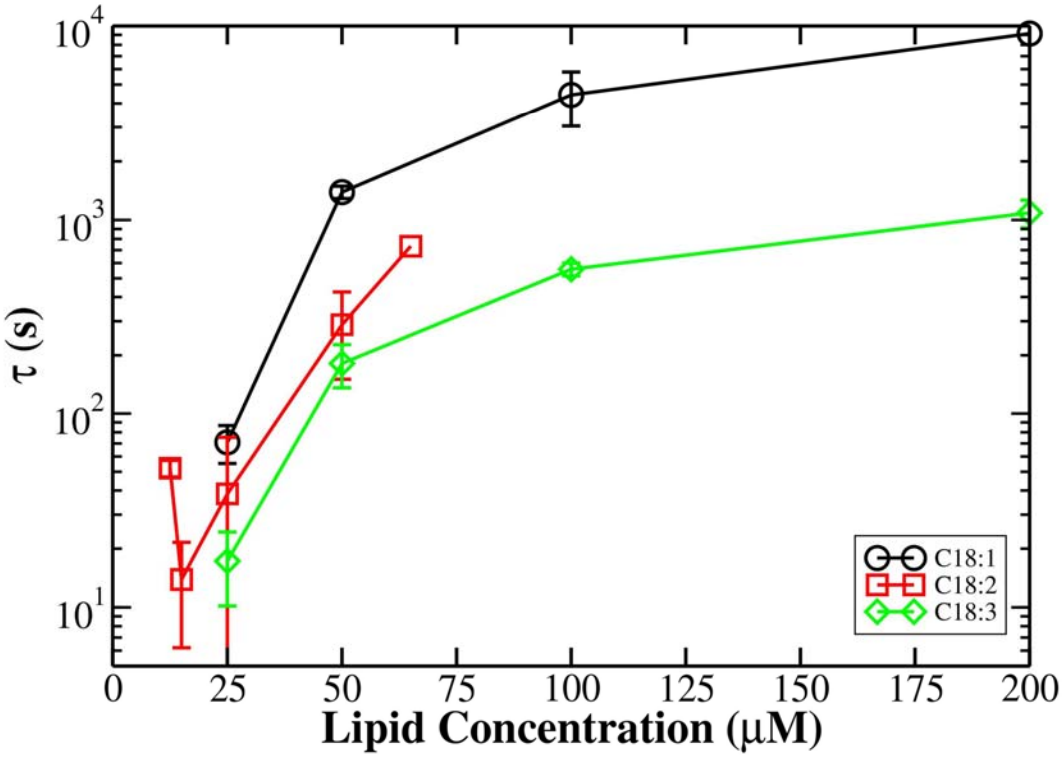

FIGURE 5: τ versus lipid concentration for diC18:1PC, diC18:2PC, and diC18:3PC showing that τ becomes larger as the lipid concentration is increases.

In Figure 6 τ is plotted against acyl chain length. A large slope was observed for chain lengths between diC14:1PC, diC16:1PC, and diC18:1PCs. Beyond that, it appeared that an additional two carbons did not significantly increase the τ for any of the lipid concentrations ranging from 12.5 μM through 100 μM. τ was also plotted against bilayer thickness in Figure 7. The slopes were very comparable to those of Figure 6. The graphs appear similar because an increase in chain length by the addition of two carbons to the acyl chain results in a proportional increase in bilayer thickness. From the shortest chain lipid to the longest chain, there were four orders of magnitude difference in τ at lipid concentrations of 25 μM and 50 μM, which is more significant than in the 18 chain lipid series.

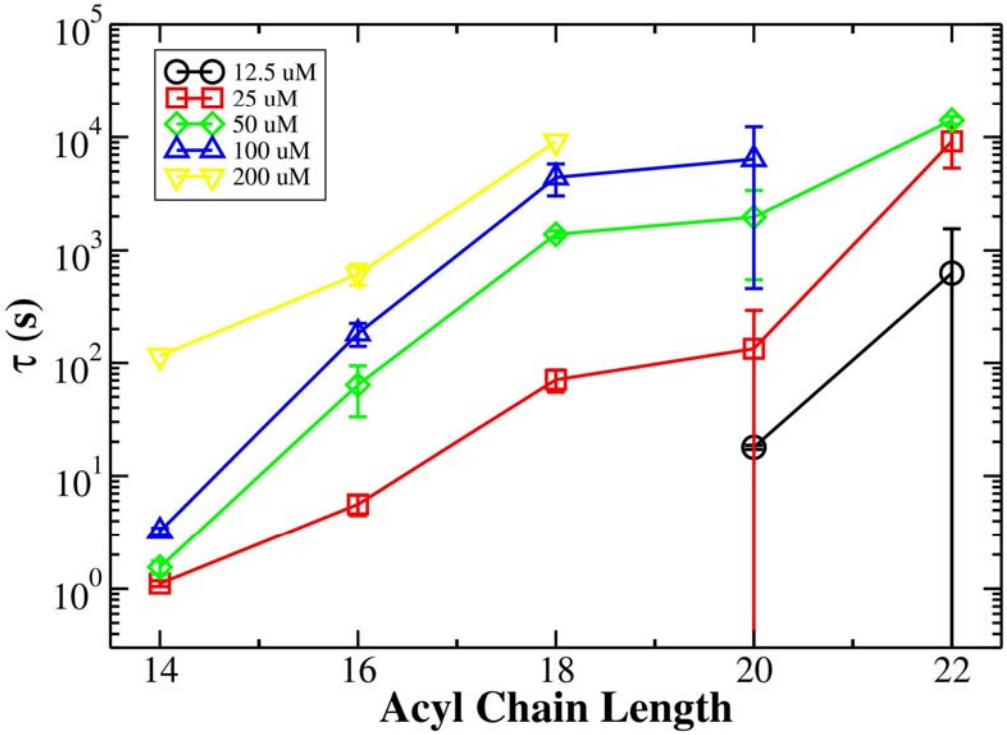

FIGURE 6: τ as a function of chain length. The graph shows an increase of log τ for all lipid concentrations, from the shortest chain length of 14 carbons up to 18 carbons.

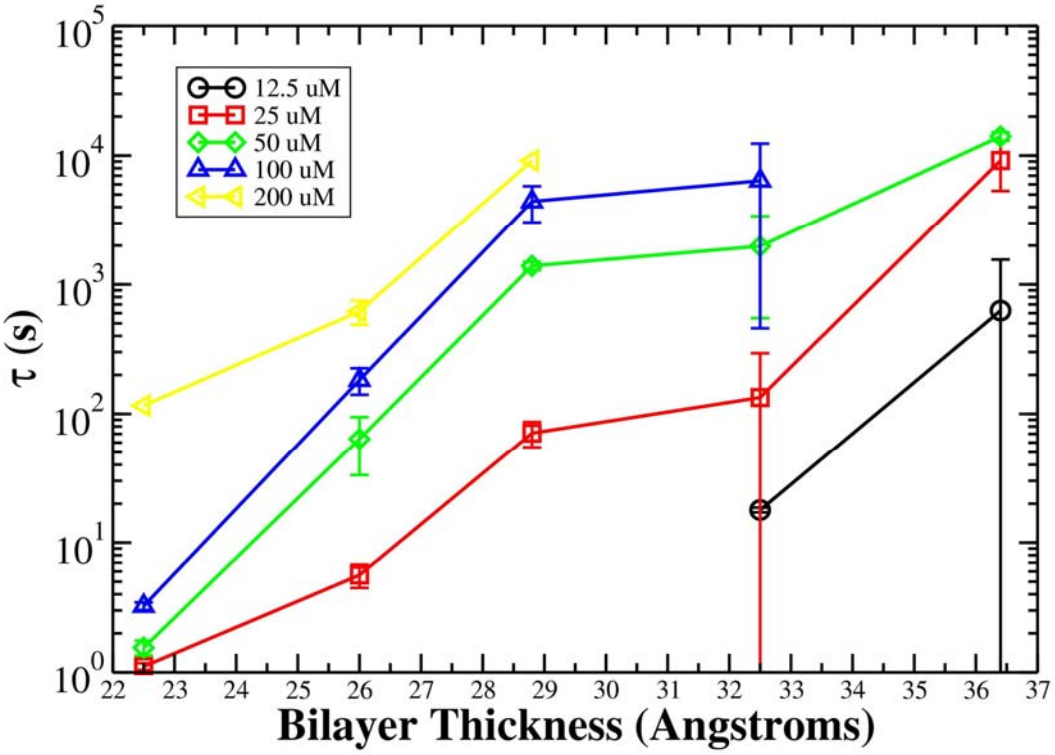

FIGURE 7: τ as a function of bilayer thickness. The graph shows an increase of τ that parallels the same trend as the previous graph. The identical trend is due to the fact that the bilayer thickness is proportional to acyl chain length.

Increasing bilayer thickness in the lipid series diC18:1PC, diC18:2PC, and diC18:3PC also increases τ as shown in Figure 8. Bilayer thickness decreases as lipid acyl chain unsaturation increases. The bilayer thickness increase between diC18:2PC and diC18:3PC was minimal in comparison to diC18:1PC and diC18:2PC. However, the overall trend was the same as in the previous plot: as bilayer thickness increased so did τ, exponentially. Slopes for all lipid concentrations seem similar for the 18 chain lipid series compared to those of the diC14:1PCs through diC22:1PCs. This second series had a one order of magnitude difference in τ between diC18:3PC and diC18:1PC.

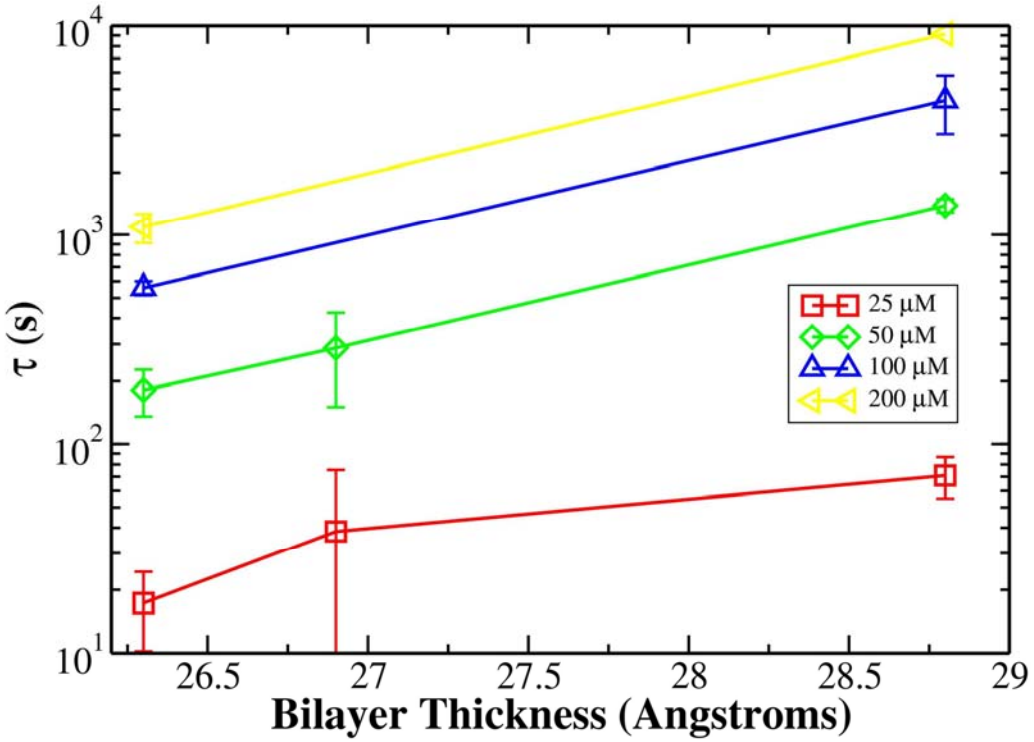

FIGURE 8: τ as a function of bilayer thickness for diC18:1PC, diC18:2PC, and diC18:3PC vesicles for lipid concentrations ranging from 25 μM, 50 μM, 100 μM, and 200 μM. Bilayer thickness is largest for the least number of unsaturations.

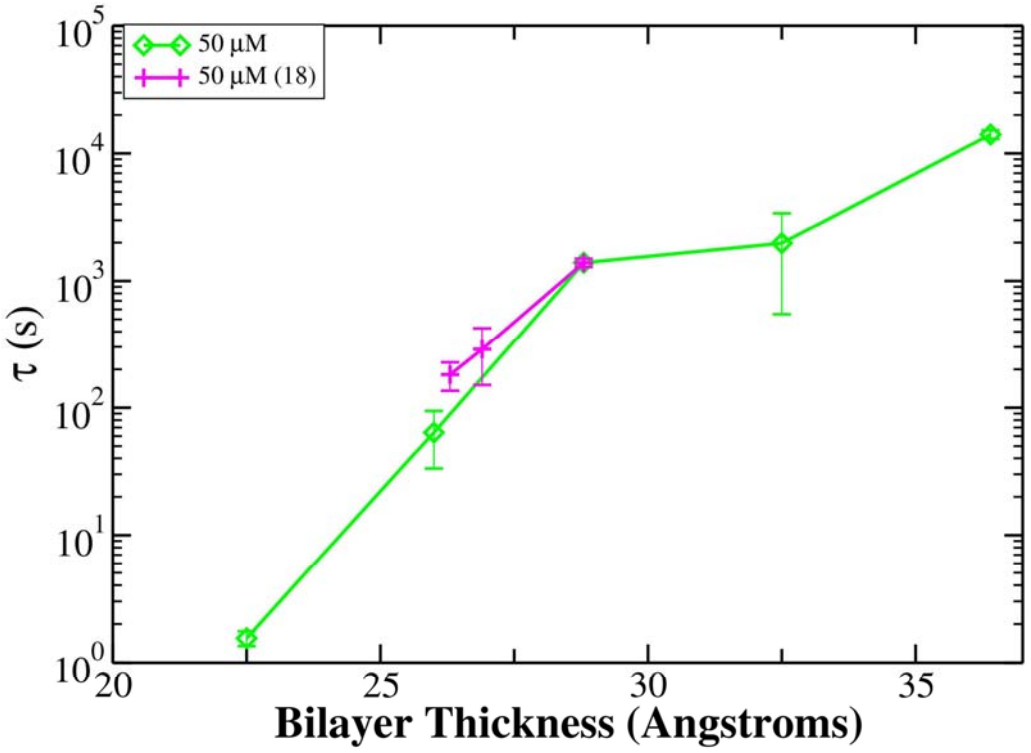

FIGURE 9: τ plotted against bilayer thickness for both lipids series are shown, at 50 μM lipid.

In Figure 10, τ was plotted against apparent *intrinsic* vesicle permeability ($P_{fapp)}$ to compare the permeability of a membrane to water with the rate of dye efflux. This gives insight into how permeability relates to the potential for leaking of vesicles. From the data collected by Olbrich (15) (values listed in table 2), water permeability increases with more unsaturations. What they found was a relatively modest increase in P_{fapp} with mono- and dimono-unsaturation, but additional cis-double bonds resulted in a much more permeable membrane. A negative slope shows that τ decreases as the P_{fapp} increases. Intrinsic vesicle permeability was higher for 18:1 than 18:3 Olbrich (15), but the P_{fapp} values of diC18:1PC, diC18:2PC, and diC18:3PC are actually rather close. So, indeed, as the unsaturation of the acyl chain increases, the resultant effect is an increase in dye leakage. δ-Lysin augmented the intrinsic lipid permeability.

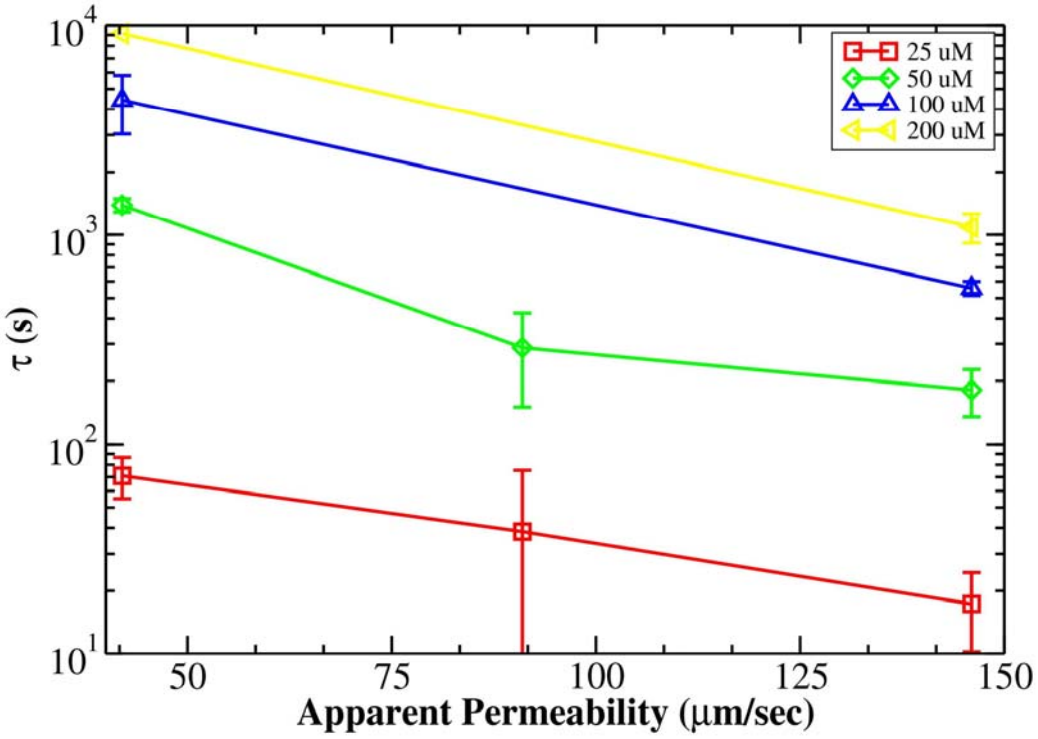

FIGURE 10: Variation of τ as a function of apparent (intrinsic) permeability of the vesicle membranes. A negative slope shows that increasing intrinsic permeability increases the rate of carboxyfluorescein efflux, induced by δ-lysin.

Figure 11 shows τ plotted against bending elasticity for two lipid concentrations. The bending moduli (k_c) values for these lipids were taken from Rawicz *et al*. (14) (data listed in Table 4). The first three points on each curve correspond to the lipids diC18:3PC, diC18:2PC, and diC18:1PC. The far right points are for diC22:1PC. The overall trend indicates that there is a correlation of the bending ability of the membrane with the rate of dye efflux. Dye efflux rates were faster from vesicles made of lipids with two or three unsaturations on the acyl chains, but that also corresponds to the two thinner membranes. The membrane can bend more easily when there are at least two unsaturations.

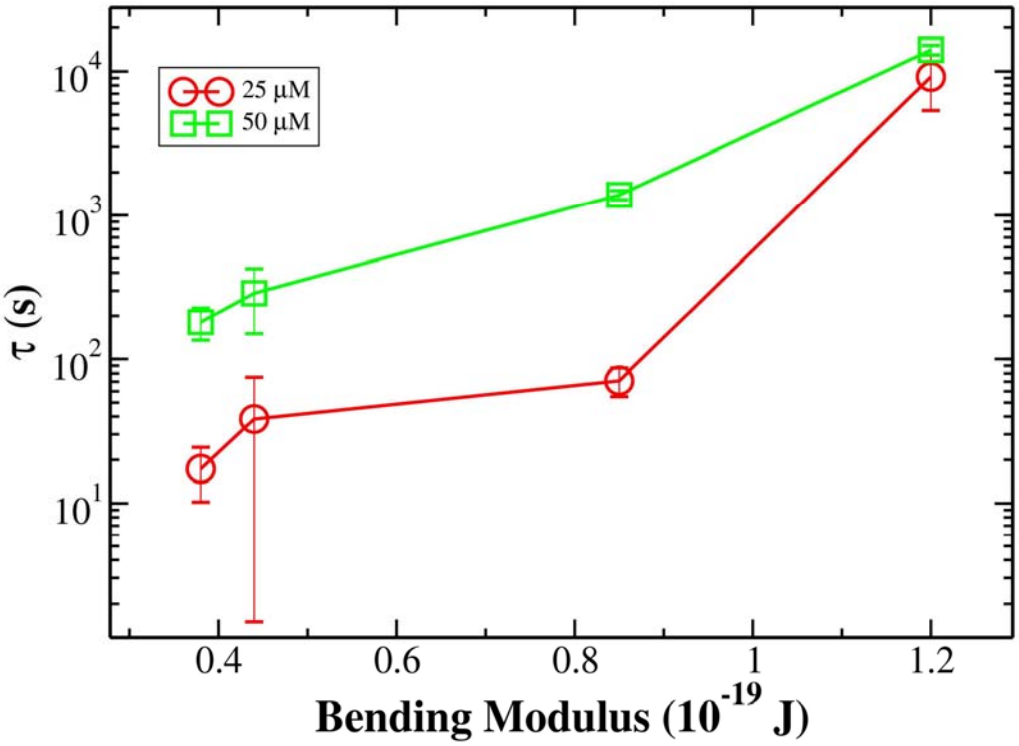

FIGURE 11: τ for the carboxyfluorescein efflux as a function of the bending modulus. Data is shown for lipid concentrations of 25 and 50µM. The bending moduli (k_c) follow the order from left to right, diC18:3PC, diC18:2PC, diC18:1PC, and diC22:1PC (Data from table 4). The graph shows that diC18:2PC induced dye efflux faster than diC18:1PC.

Figure 12 shows τ plotted against the elastic moduli (K_A) in order to investigate whether there is a relationship between the stretching ability of the membrane and the rate of dye efflux. K_A values are listed in Table 3. The x-axis corresponds to the K_A values in the following order: diC18:3PC, diC18:2PC, di22:1PC, and diC18:1PC. The slope between K_A values from 244 mN/m to 263 mN/m is a steady positive. However, as K_A increases from diC22:1PC (263 mN/m) to diC18:1PC (265 mN/m), there is a steep decline in τ. Dye efflux times appear to increase a steadily up until diC22:1PC. The τ values of diC18:1PC with lipid concentration 25 μM and 50 μM do not fall below that of diC18:3PC and diC18:2PC, even though the slope falls after diC22:1PC. This suggests that for the three 18 chain lipids the rate of dye efflux continues to increase as the number of unsaturations increases. However, diC22:1PC breaks that trend by having the largest τ for carboxyfluorescein efflux. Increasing the chain length also increases the stretching modulus, yet a thicker membrane hinders dye efflux more than a thinner membrane. Therefore, no obvious trend in τ is observed when increasing stretching moduli. In addition, τ changes by 3 orders of magnitude while the stretching elasticity hardly varies. Thus, it appears unlikely that stretching of the membrane is a major factor in the rate of efflux.

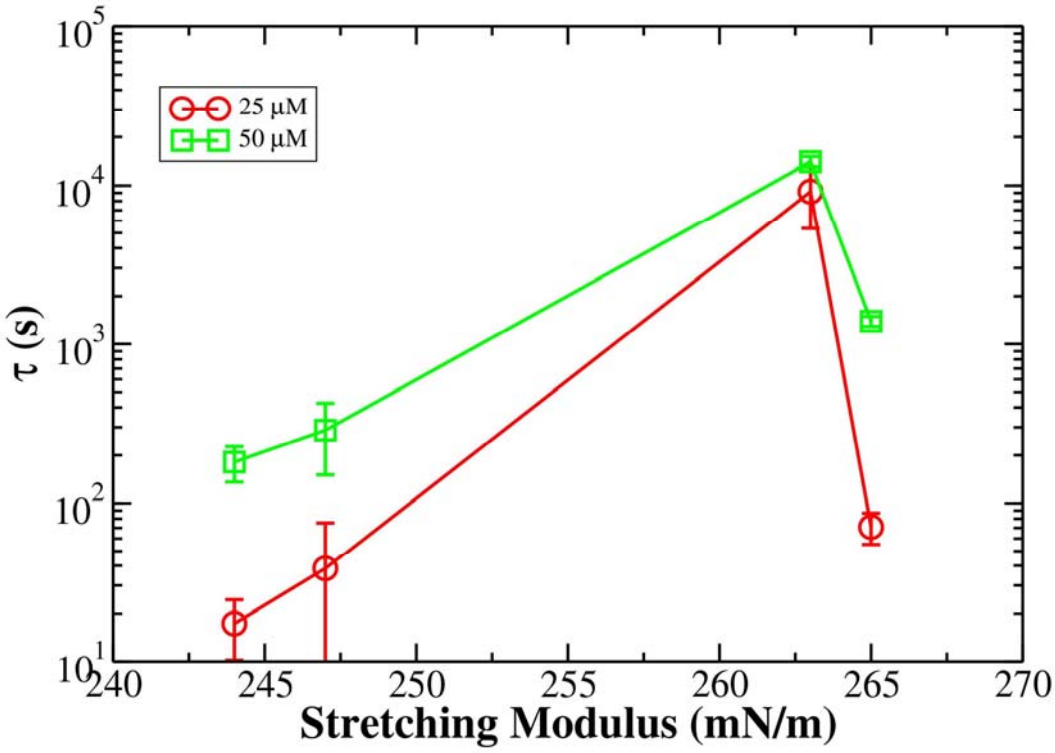

FIGURE 12: Stretching moduli in the order of these lipids: diC18:3PC, diC18:2PC, diC22:1PC, and diC18:3PC. Slopes did not increase much with increasing unsaturation indicating that efflux rates did not increase significantly with increasing unsaturation. Dye efflux time was longer for diC22:1PC.

In Figure 13, τ was plotted against T-T_m, where T is 21˚C, to assess the effect of free volume (eq 2). The order of points from left to right is diC22:1PC, diC20:1PC, diC18:1PC, diC16:1PC, diC14:1PC, diC18:2PC, and diC18:3PC. T-T_m values increase as the chain length decreases, however they also increase as the number of acyl chain unsaturation increases. τ decreases continuously from diC22:1PC through diC14:1PC (when T-T_m reaches 70˚C), but increases afterwards. Both lipid concentrations of 25 μM and 50 μM show the same effect. The efflux rate for two and three unsaturations for the 18 chain lipids do not fall below diC16:1PC. However, the rate of dye efflux did decrease again between diC18:2PC, and diC18:3PC, shown as the last two points.

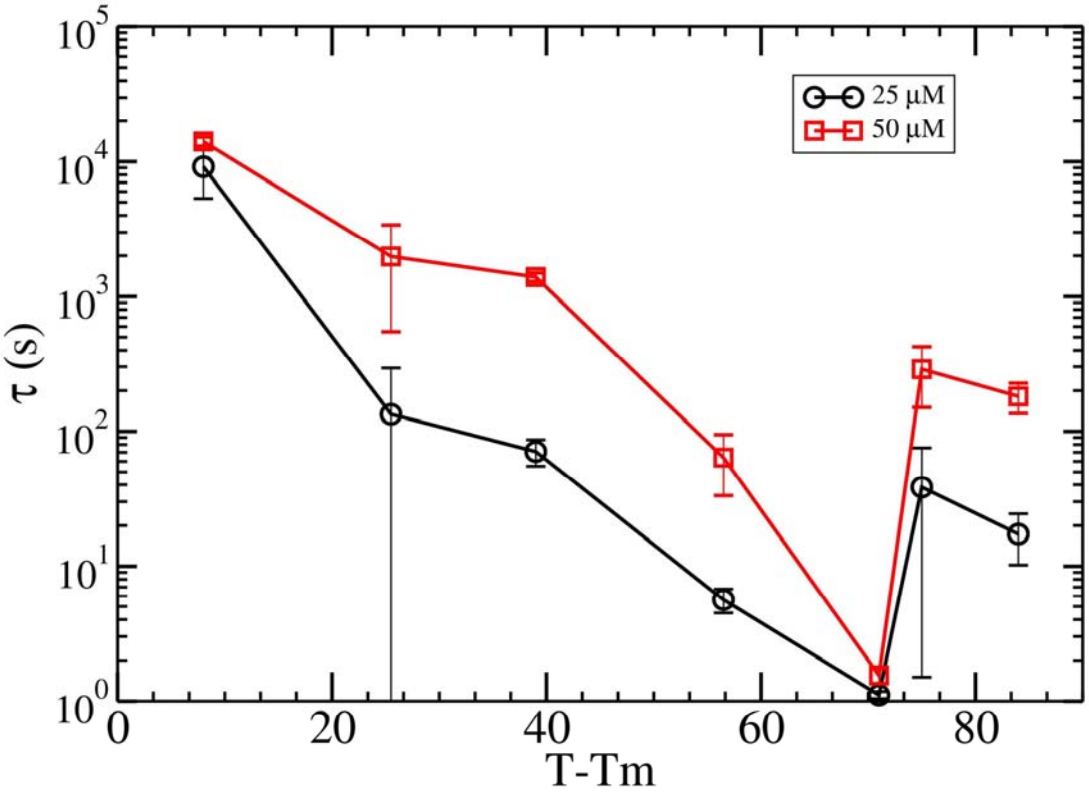

FIGURE 13: τ as a function of T-T_m. T_m values taken from Hinderliter *et al.* (19). The order of points from left to right is diC22:1PC, diC20:1PC, diC18:1PC, diC16:1PC, diC14:1PC, diC18:2PC, and diC18:3PC. τ decreases until 70˚C, and it then increases beyond diC16:1PC. Subsequently τ decreases again for diC18:3PC.

DISCUSSION

δ-Lysin is a hemolytic, amphipathic peptide that binds well to charged and neutral membranes. Because δ-lysin does not appear to rely on charge as a mechanism of binding to the membrane, it was important to study another possibility that has gained far less attention, the acyl chain and the influence it has on peptide membrane interactions. There has not been a thorough study of a lipid series that describes the effects of membrane thickness and chain unsaturation.

The effect of acyl chain composition was investigated using two lipid series: (a) diC14:1PC, diC16:1PC, diC18:1PC, diC20:1PC, and diC22:1PC; and (b) diC18:1PC, diC18:2PC, and diC18:3PC. We hypothesized that an 'effective pore' needed for δ-lysin to disrupt the membrane was dependent on one of two factors, or perhaps both, free volume and bilayer elasticity. This study was performed to determine if free volume in the hydrocarbon region was responsible for a permeable hole, or whether bilayer elasticity (bending stiffness and stretching) was the determining factor for pore formation. The experiments were performed by the addition of δ-lysin to carboxyfluorescein-containing lipid vesicles in order to induce dye efflux. Each sample was composed of lipids with varying acyl chain composition.

The effect of free volume was assessed by studying the variation of τ with T-T_m. Also, free volume was studied using data collected from Olbrich *et al*. (15), along with the lateral diffusion coefficient (19). Both stretching moduli and lateral diffusion coefficients remained very similar for the series of lipids used. This indicated that there was little to no correlation with free volume and the rate of carboxyfluorescein efflux. Therefore, little change would be expected for dye efflux with the homologous lipid series diC14:1PC, diC16:1PC, diC18:1PC, diC20:1PC, and diC22:1PC. According to the free volume theory, varying this lipid series

corresponds to varying $T_{m,}$ while keeping the temperature constant (eqs 1-2). As a result, if free volume were to be a dominating factor for insertion of δ-lysin, this lipid series should not exhibit dramatic changes in dye efflux rates and increasing *T-Tm* would have a monotonic variation in τ. The results from this lipid series revealed faster efflux kinetics for the short chain lipids, and as the acyl chain increased carboxyfluorescein efflux showed a significant rate decrease indicated by larger τ values. There is not a monotonic variation in τ with increasing $T-T_{m,}$ as shown in Figure 13. Therefore, it appears that free volume is not the most important factor for peptide insertion.

Stretching of the membrane moves the lipids laterally, allowing formation of a transverse hole for the peptide to insert into the membrane, as shown in Figure 14. The ability for a membrane to stretch is measured by the stretching modulus. These values did not vary much (Table 3). However, there was a 3 order of magnitude difference in τ shown in Figure 11, which indicates that dye efflux rates are dependent on other factors. Also, in order for stretching to be an essential part for peptide insertion, there should be a monotonic variation in τ. However, there was not a monotonic variation in τ as seen in Figure 12. Additionally, τ values did not significantly vary with stretching moduli corresponding to the 18 chain unsaturated lipids alone. Instead, it increased most for the stretching moduli that corresponded to the longest chain length. It seems that stretching does not play a major role in peptide-induced dye efflux. Because both free volume and bilayer stretching appear to play minor roles in peptide insertion, creating a transverse hole of adequate size is probably not necessary for dye efflux. Consequently, it appears that the *barrel stave* model is not the mechanism at work, because the probability of a peptide aggregate to insert in the membrane should be proportional to the probability of formation of an adequate sized, transverse hole across the bilayer.

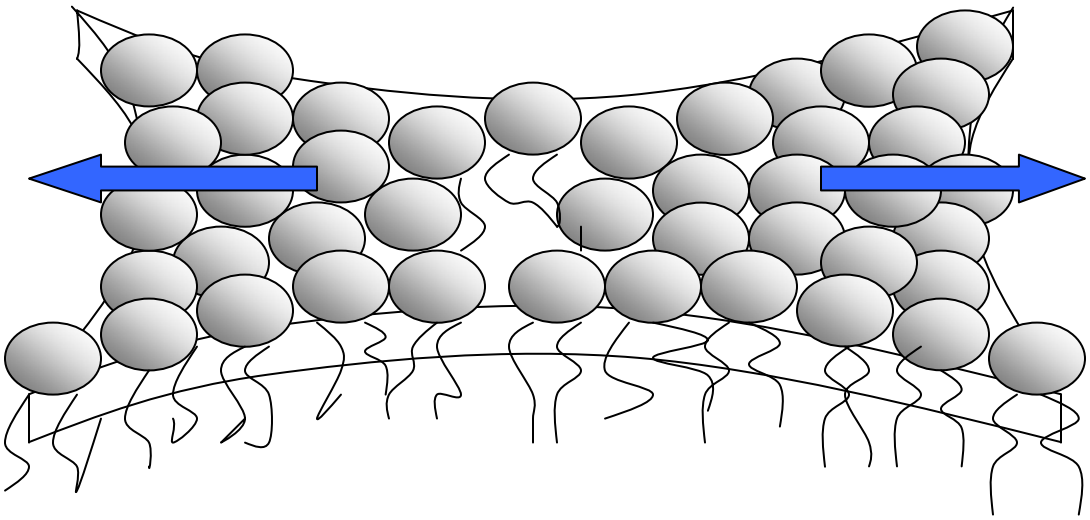

FIGURE 14: Membrane stretching. The circles represent the phospholipid headgroups and their acyl chains. The arrows show the direction of the stretch that occurs with the lipid bilayer. Away from the direction of pull is the transient opening located in the center the membrane.

The thickness of the membrane appeared to be very important for dye efflux rates. For both lipid series, the longer acyl-chain lipids caused a decrease in efflux rates. Based on the data collected, the 18 chain lipids had an average of one order of magnitude difference in τ from diC18:3PC, the shortest lipid in this series, to diC18:1PC, the longest chain. On the other hand, the first lipid series revealed a larger change in τ. From diC14:1PC to diC22:1PC, there was a four order magnitude decrease in the efflux rates. If the peptide translocated to the inner side, it was expected that the thickness of the bilayer would influence the peptide traveling distance across the membrane. The thicker the membrane is, the lower the probability that the peptide will travel across the membrane. It is also possible that the effect is not on the peptide translocation probability, but on the carboxyfluorescein efflux rate itself, occurring while the peptide perturbed the membrane. However, it was not predicted how great the effect would be, which apparently is quite significant.

Pore formation occurs more easily with bilayers that have greater flexibility (lower bending stiffness). As chain length increases the lipid bilayer thickens, and the flexibility of the membrane decreases, which has been shown by measurements taken for bilayer elastic bending moduli of twelve PC membranes (14). Saturated and monounsaturated PC exhibit this trend as the acyl chain lengthens, but a dramatically greater bending elasticity is observed for polyunsaturated PC (14). Both increasing unsaturation of the acyl chain and decreasing membrane thickness cause a significant increase in bilayer elasticity. Therefore, there is a strong correlation between bending stiffness and bilayer thickness, which is expected from theory. Thus, it was due to this correlation that we decided to test our hypothesis with the second lipid acyl series diC18:1PC, diC18:2PC, and diC18:3PC as well.

The bending moduli data taken from Rawicz *et al.* (14) show that increasing unsaturation causes the membrane to bend more easily, and bending becomes increasingly difficult as acyl chain increases. The steep slopes shown in Figure 11 between diC18:3PC and diC22:1 indicated that dye efflux rates dramatically decreased as the bending modulus increased.

The bending moduli and stretching moduli plots against τ strongly supported the hypothesis that membrane thickness is an important contributor to the mechanism of δ-lysin function. Initially, it was obvious only that thicker membranes required more time for dye to come out of the vesicle. Yet careful analysis of the bending and stretching moduli revealed that, for bending, the rate of efflux follows the trend for unsaturation and membrane thickness. However, stretching of the membrane did not correlate with dye efflux rates. Apparently, as the stretching capacity of the membrane decreases, it is not solely dependent on unsaturation as was initially thought. DiC22:1PC membranes can stretch more easily than diC18:1PC. Yet the rates of dye efflux were dramatically higher for the 18 chain lipids, suggesting that thickness of the membrane matters more than stretching ability. Bending correlates with unsaturation and thickness, which in turn should result in a mechanism that favors peptide action that can bend the membrane, or work better when the membrane bends easily for it to insert. One important observation from Figure 11 was that τ increases monotonically with the bending modulus (k_c) independently of whether k_c is changed by altering the chain unsaturation of the chain length of the lipid. δ-Lysin can more easily move into the lipid bilayer when there are more unsaturations because the membrane is more bendable, but when the membrane becomes thicker, the bending elasticity diminishes significantly. If the membrane bends easily, then the amphipathic structure of δ-lysin should be able to bind to the surface of the membrane due to the hydrophobic effect, and sink as a 'wedge' into the lipid bilayer. This model is consistent with the s*inking raft* model,

but it also supports the *toroidal hole* model because curvature of the membrane is also induced for this mechanism.

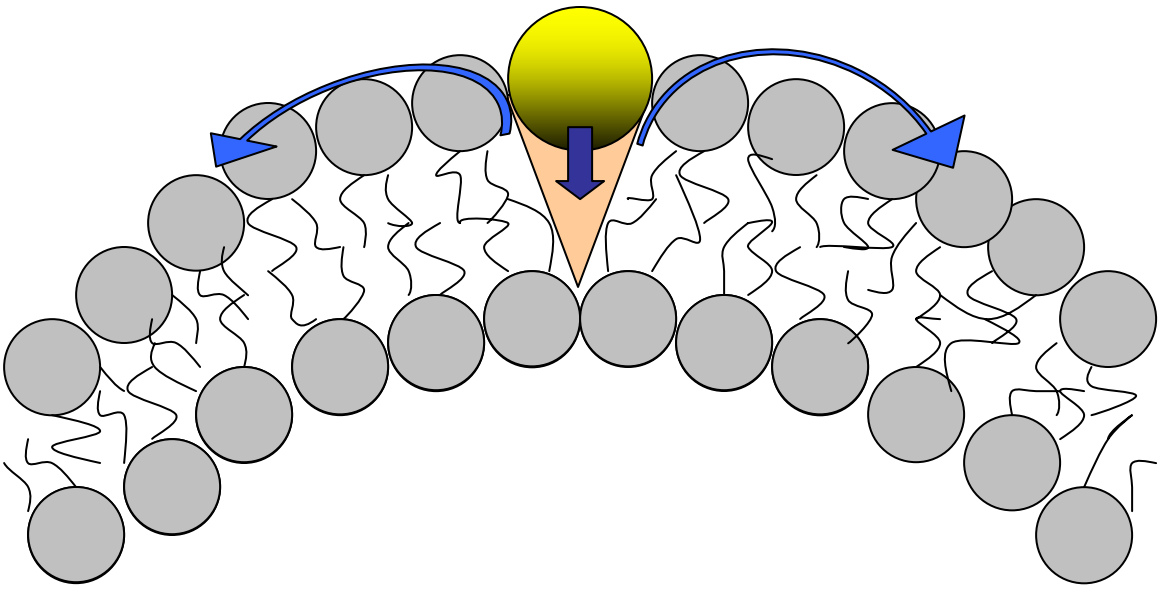

FIGURE 15: Membrane bending. The yellow faded circle represents δ-lysin. The lipid bilayer is shown by the gray circles for the phospholipid headgroups and acyl chains. A blue arrow below δ-lysin represents the direction of decent into the lipid bilayer towards hydrophobic region. Curved arrows along the phospholipid headgroups demonstrate the bending of the membrane surface resulting in the "wedge" formed in the membrane shown in orange.

We predicted that intrinsic permeability of the membrane would also match with the rates of dye efflux, and indeed they did. Only diC18PCs data were available, so this remains more an observation subsequently made for unsaturated lipids. Membranes appear to be more permeable to water and dye efflux does follow the trend of increasing leakage rates. It appears that permeability is also an effect of membrane thickness, but distinguishing that against level of unsaturation will require further investigation.

Along with observations made for acyl chain composition, lipid concentration also affected efflux rates. As lipid concentration increased, which for these experiments were doubled each time, the underlying effect was a dilution of the peptide on the surface of the membrane. Each time the lipid concentration doubled, the number of peptides that were able to collect per vesicle decreased. These observations lead to the conclusion that, indeed, aggregates are necessary for δ-lysin to function effectively. However the exact aggregate size was not determined. Only the trend was noted.

Taking all data together, the main cause for increase in dye leakage appears to be the bendability of the membrane, which depends on bilayer thickness. τ does not vary monotonically with stretching elasticity or free volume. So the mechanism of δ-lysin does not appear to involve the *barrel stave* model. Instead, τ varies monotonically with the stretching modulus and bilayer thickness. Thus, the *sinking raft* model or *toroidal hole* model seem to account for the action of δ-lysin. Ultimately, any model that can induce curvature in the membrane due to bending can be a possible mechanism.

It seems necessary then to further this study by challenging the question of whether it is more thickness of the membrane or level of unsaturation alone to be the cause of membrane identification and function of certain peptides. Perhaps it is both. Also, because the aggregate

size is unknown, this might be another area to study. Also, because the aggregate size is unknown, this might be another area to study. Additionally, studying the interaction between δ-lysin and lipid membranes composed of several lipids with different degrees of unsaturation may allow determination of an optimum membrane composition.

REFERENCES

1. Marshall, S H., and Arenas, G. (2003) Antimicrobial peptides: A natural alternative to chemical antibiotics and a potential for applied biotechnology, *Elec. J. Biotech*. 6, 271-284.

2. Bechinger, B. (1999) The structure, dynamics and orientation of antimicrobial peptides in membranes by multidimensional solid-state NMR spectroscopy, *Biochim. Biophys. Acta 1462*, 157-183.

3. Zasloff, M. (2002) Antimicrobial peptides of multicellular organism, *Nature 415*, 389-395.

4. Hancock, R. E. W., Diamond, G. (2000) The role of cationic antimicrobial peptides in innate host defences, *Trends Microbiol. 8,* 402-10.

5. Hancock, R. E. W. (2001) Cationic peptides: effectors in innate immunity and novelantimicrobials, *The Lancet 1*, 156-164.

6. Matsuzaki, K. (1999) Why and how are peptide-lipid interactions utilized for self defense? Magainins and tachyplesins as archetypes, *Biochim. Bhiophys. Acta 1462*, 1-10.

7. Shai, Y. (1999) Mechanism of the biding, insertion and destabilization of phospholipids bilayer membranes by α-helica antimicrobial and cell non-selective membrane-lytic peptides, *Biochim. Biophys. Acta 1462*, 55-70.

8. Pokorny, A., Birckbeck, T. H., and Almeida, P. F. F. (2002) Mechanism and Kinetics of δ-Lysin interaction with phospholipids vesicles, *Biochemistry 41*, 11044-11056.

9. Wade, D. Bowman, A., Wahlin, C. M., Drain, Andreu, D., Boman H. G., and Merrifield R. B. (1990) All-D amino acid-containing channel-forming antibiotic peptides, *Biochemistry 87,* 4761-4765.

10. Mchaourab, H. S., Hyde, J. S., and Feix, J. B. (1994) Binding and state of aggregation of spin-labeled cecropin AD in phospholipids bilayers: effects of surface charge and fatty acyl chain length, *Biochemistry 33*, 6691-6699.

11. Raghuraman, H., and Chattopadhyay, A. (2004) Influence of lipid chain unsaturation on membrane-bound melittin: a fluorescence approach, *Biochim. Biophys. Acta 1665*, 29-30.

12. Monette, M., and Lafleur, M. (1996) Influence of Lipid oChain Unsaturation on Melittin-Induced Micellization, *Biophys. J. 70* , 2195-2202.

13. Nicol, F., Nir, S., and Szoka Jr. F.S. (2000) Effect of phospholipids composition on an amphipathic peptide-mediated pore formation in bilayer vesicles, *Biophs. J. 78*, 818-829.

14. Rawicz, W., Olbrich, K. C., McIntosh, T., Needham, D., and Evans, E. (2000) Effect of Chain Length and Unsaturation on Elasticity of Lipid Bilayers, *Biophys. J.* 79, 328-339.

15. Olbrich, K., Rawicz, W., Needham, D., and Evans, E. (2000) Water Permeability and Mecahnical Strength of Polyunsaturated Lipid Bilyers, *Biophs. J.* 79, 321-327.

16. Cohen, M. H. and Turnbull, D. (1959) Molecular Transport in liquids and Glasses. *J. Chem. Phys. 31*, 1164-1169.

17. Vretas. J. S., Duda, J. L., and Ling, H. –C. (1985) Free-Volume Theories for Self Diffusion in Polymer-Solvent Systems. I. Conceptual Differences in Theories. *J. Polym. Sci. 23*, 275-288.

18. Vaz, W. L., Clegg, R.M., and Hallmann, D. (1985). Tanslational diffusion of lipids in liquid crystalline phase phosphatidylcholine multibilayers. A comparison of experiment with theory. *Biochemistry 24*, 781-786.

19. Hindreliter, A., Biltonon, R. L., and Almeida, P. F. F. (2004) Lipid Modulation of Protein-Induced Membrane Domains as a Mechanism for controlling Signal Transduction, *Biochemistry 43*, 7102-7110.

20. Almeida, P. F. F., Vaz, W. L. C., and Thompson, T. E. (1992) Lateral diffusion in the liquid phases of dimyreistoylphosphatidylcholine/cholesterol lipid bilayers: a free volume analysis. *Biochemistry 31*, 6739-6747.

21. Allende, D.,Vidal A., Thomas, J. M. (2004) Jumping to rafts: gatekeeper role of bilayer elasticity, *Trends Biochem. Sci. 29,* 325-330.

22. Arranda, F. J.,Teruel, J. A., Ortiz,A. (2003) Interaction of a synthetic peptide corresponding to the N-terminus of canine distemper virus fusion protein with phospholipids vesicles: a biophysical study, *Bhiochim. Biophys. Acta 1618*, 51-58.

23. Bhakoo, M., Birkbeck, T. H., Freer, J. H. (1982) Interaction of *Staphylococcus aureus* δ-Lysin with Phopholipid Monolayers, *Biochemistry 21,*6879-6883.

24. Bechinger, B. (2000) Understanding peptide interactions with the lipid bilayer: a guide to membrane protein engineering, *Curr. Opin.Chem. Biol. 4*, 639-644.

25. Bernard, E., Faucon J., Dufourcq, J. (1982) Phase separation induced by melittin in negatively-charged phopholipid bilayers as directed by fluorescence polarization and differential scanning calorimetry, *Biochim. Biophys. Acta 688*, 152-162.

26. Dufourc, E. J., Bonmatin, J.l, Dufourcq, J. (1988) Membrane structure and dynamics by 2H- and 31P-NMR. Effects of amphipatic peptidic toxins on phospholipids and biological membranes, *Biochimie 71*, 117-123.

27. Lafleur, M., Faucon, J., Dufourcq, J. Pézolet, M. (1989) Peterbation of binary phopholipid mixtures by melittin: A fluorescence and Raman spectroscopy study, *Biochim. Biophys. Acta 980*, 85-92.

28. Li, W., Nicol, F., Szoka Jr., F. C. (2004) GALA: a designed synthetic pH responsive amphipathic peptide with applications in drug and gene delivery, *Adv. Drug Del. Rev. 56*, 967-985.

29. Wu, M., Maier, R. B., Hancock, R. E. W. (1999) Mechanism of interaction of different classes of cationic antimicrobial peptides with planer bilayers and with the cytoplasmic membrane of *Escherichia coli*, *Biochemistry 38*, 7235-7242.